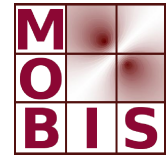




SpezialForschungsBereich F 32



Karl-Franzens Universität Graz
Technische Universität Graz
Medizinische Universität Graz



Spectroscopic 16 channel magnetic induction tomograph: The new Graz MIT system

H. Scharfetter A. Köstinger S. Issa

SFB-Report No. 2007-010

December 2007

A-8010 GRAZ, HEINRICHSTRASSE 36, AUSTRIA

Supported by the
Austrian Science Fund (FWF)

FWF Der Wissenschaftsfonds.

SFB sponsors:

- **Austrian Science Fund (FWF)**
- **University of Graz**
- **Graz University of Technology**
- **Medical University of Graz**
- **Government of Styria**
- **City of Graz**



Spectroscopic 16 channel magnetic induction tomograph: The new Graz MIT system

H. Scharfetter, A. Köstinger and S. Issa

¹ Institute of Medical Engineering, Graz University of Technology, Kopernikusgasse 12, Graz, Austria

Abstract— Frequency differential magnetic induction tomography allows the reconstruction of images of relative conductivity spectra with the aid of magnetic AC fields and coil arrays. We describe a new 16-channel hardware with an analog bandwidth of 50 kHz – 1.5 MHz which covers a good part of the β -dispersion of many tissues. At each acquisition time 8 of the 16 excitation coils are simultaneously driven by individual power amplifiers with up to 3 A_{ss} at multiple frequencies. These amplifiers are configured as current sources so that every coil termination is high enough so as not to perturb the field of all other coils. For encoding the excitation coils their individual carrier frequencies differ by 200 - 500 Hz. In this way every excitation frequency is split into 8 subcarriers within a bandwidth of 1.6 - 4 kHz so that they can be approximately considered as a single peak in the comparatively flat tissue spectrum. The magnetic fields are received by 16 planar gradiometers and the induced voltages are amplified by low-noise amplifiers before being fed into the ADC. The real and imaginary parts of the received signals are extracted efficiently with FFT. The SNR is reduced by a factor of 5 when compared to the theoretical limit of our previous single-excitation system but due to the much higher acquisition speed drifts and physiological noise are considerably lower.

Keywords— Magnetic induction tomography, multifrequency hardware, coil system.

I. INTRODUCTION

Magnetic induction tomography (MIT) [1],[2],[3] aims at the reconstruction of the passive electrical properties within an object from the measurement of magnetic field perturbations. MIT requires an alternating magnetic excitation field \mathbf{B}_0 to be coupled from an array of transmit (TX) coils to the object under investigation. Changes $\Delta\kappa$ of the complex conductivity $\kappa = \sigma + j\omega\epsilon_0\epsilon_r$ and changes $\Delta\mu_r$ of the relative magnetic permeability μ_r in the target region cause a field perturbation $\Delta\mathbf{B}$ due to the induction of eddy currents and magnetic dipoles in the object under investigation. The perturbation field is then measured via an array of receiver (RX) coils. Usually a vector $\Delta\mathbf{u}$ of relative voltage changes $\Delta V_i/V_{0,i}$ is acquired from all possible independent drive-receive combinations indicated by the index i . ΔV_i is the voltage change and $V_{0,i}$ is the induced voltage in one receiver coil in the absence of a perturbation.

Previous MIT systems developed for medical applications used frequencies of several MHz to increase the perturbation signal produced by eddy currents in low conductivity tissues, i.e. 20 MHz, [2], 10 MHz [1], 4 MHz [4]. In contrast, for process tomography the systems are working at lower frequencies because the materials are usually ferromagnetic or highly conductive. [3] describes a system using 500 kHz to detect conductive or ferromagnetic particles. In a more recent work, [5] a new system using 5 kHz for the detection of molten steel flow is presented. In [6] a scanning system was published which operates at very low frequencies (11.6 kHz),

Our own group has developed the first multi-frequency system which covers the spectrum between several tens of kHz up to 1 MHz [7]. Such a system allows the reconstruction of frequency differential and spectral images [8]. Based on [9] the frequency range was chosen as the result of a tradeoff between sensitivity considerations and the aim to cover a good part of the β -dispersion of most human tissues. The prototype employed 14 RX and 1 TX coil. Therefore, in order to obtain projections from 16 different directions, the sample had to be rotated in steps of 22.5°. This article describes a new parallel hardware with 16 RX and 16 TX coils and the capability of single shot spectroscopic imaging.

II. METHODS AND RESULTS

A. Coil system

The coil system is depicted in Fig. 1. It consists of 16 transmit-receive units (TRXU) which are arranged in two groups in form of an upper and a lower ring with 8 units per ring. Each TRXU consists of a shielded solenoid TX coil and a receiving planar gradiometer (PGRAD) which is mounted with its face parallel to the face of the TX coil. The gradiometer is adjusted with respect to the TX coil so that it receives the minimum net magnetic flow from. The normal distance from the TX coil is approximately 3 cm. The data of the coils are the same as published in our previous prototype [7]: TX coil: 8 windings, diameter 10cm, 11.2 μ H. PGRAD: 2 x 40 spiral windings, 95 μ H, 16.7 Ω , resonance frequency 1.56 MHz.

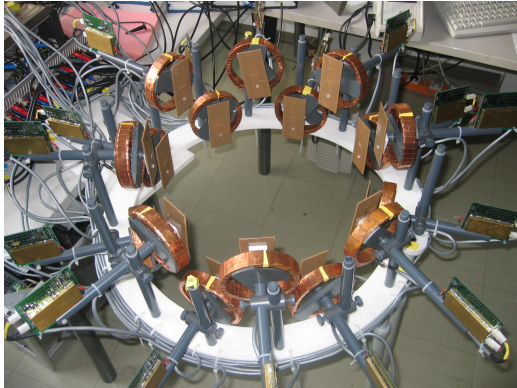


Fig. 1: photograph of the coil system. The 16 TRXUs are arranged in two ring-shaped groups on two different levels.

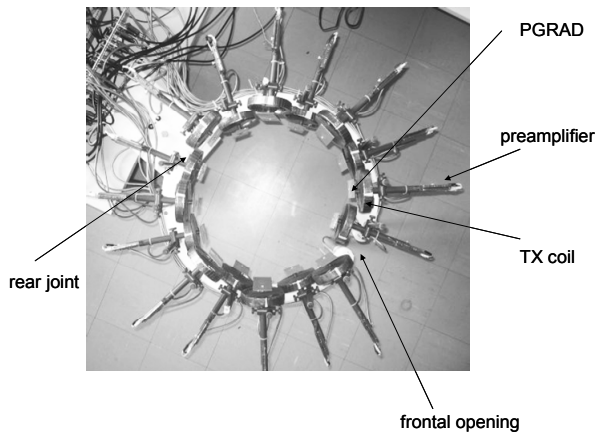


Fig. 2 : Top view of the coil system, showing the mechanism for opening the ring (joint, opening) and the components of the TRXUs.

Each TRXU is mounted on a plastic support which can be shifted up/down and along the radius of the ring. Moreover each unit can be horizontally tilted through an angle of +/- 20 deg so that there is considerable flexibility in localization and orientation of the coils.

The ring is split into two halves and has a joint (see Fig. 2) so that it can be opened. In this way a person can easily enter the system and afterwards it is closed again for the measurements. As in our previous systems we have a reference coil which provides the reference phase for synchronous demodulation (not shown here). This coil consists of only one single turn of wire which is wound on a split plastic ring in the middle plane between upper and lower TRXU group. In this way it receives approximately the same magnetic flow from all TX coils at the same time.

B. Excitation patterns and signal generation

Fast and accurate spectroscopic imaging requires the simultaneous excitation of many, if not all coils. In the case of multifrequency imaging also all frequencies should be applied at once so as to avoid drift between the acquisitions at different frequencies. The extreme case is a multifrequency single-shot system. However, it is not possible to excite several coils simultaneously at the same frequency because then the superimposed contributions cannot be separated any more and image reconstruction fails.

Solution: For practical spectroscopic purposes the different measurement frequencies can usually be separated by at least several tens of percent. It is now possible to label the n different exciters by splitting up each of the individual excitation carriers in n -tuples of closely neighboring frequencies (multiple subcarrier encoding MUSEN). The frequency interval between the subcarriers must be chosen such that on the one hand it allows for sufficient separation of the different excitation signals and, on the other hand, the dispersions of the tissue conductivities can be neglected within the bandwidth of the individual subcarrier-packages. In practice e. g. a spacing by several 100 Hz may be adequate.

This concept is illustrated in Fig. 3 for three excitation coils and two frequencies in the β -dispersion range of typical tissues. As sketched in Fig. 3A the two frequencies are chosen such that the contrast between two tissues is significantly different and therefore allows for frequency differential imaging (see e. g. [8]). Both frequencies are split up into three subcarriers, respectively (Fig. 3B), which are assigned to the TX coils (Fig. 3C).

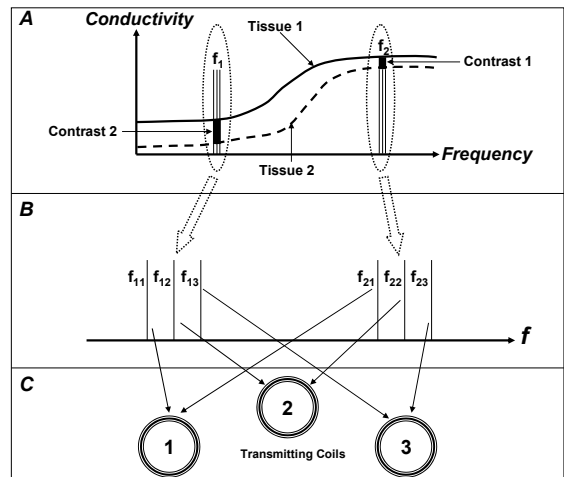


Fig. 3: multiple subcarrier encoding scheme for two carrier frequencies and 3 TX coils. A: Measurement at 2 different frequencies, B: Splitting of f_1 and f_2 into triples of 3 closely neighboring subcarriers, C: Driving of the TX coils with individual subcarriers.

At the receiver side the signals could be decoded with classical synchronous demodulation. However, the latter would require the scalar multiplication of $N \times M$ data vectors with the respective reference signals with N the number of TX channels (subcarriers), and M the number of frequencies. With $N = M = 16$ this is computationally very time-consuming, so a better alternative is to apply an FFT to the mixed signal of each RX channel and to pick out the different subcarriers from the complex spectra. This requires only 16 FFT operations which is much more efficient than 256 synchronous demodulations.

Signal generation is done by digital synthesis with LABVIEW and the resulting waveforms are output via 8 DAC-channels of two multifunction boards (NI PXI-6259).

C. Excitation drivers

The TX coils are driven by individual power amplifiers (PA19 by APEX Microtechnology) which are able to deliver up to $1.5 A_{RMS}$ of current at 100 kHz. The schematic of one driving stage is shown in Fig. 4. All drivers are configured as current sources. The reason for this design is that voltage sources would act as a low impedance termination of the TX coils which would cause severe perturbations of the magnetic field by the coils themselves. Although such perturbations could be considered in the image reconstruction algorithm this would complicate the forward modelling process by requiring explicit coil models. The use of current sources avoids this complication.

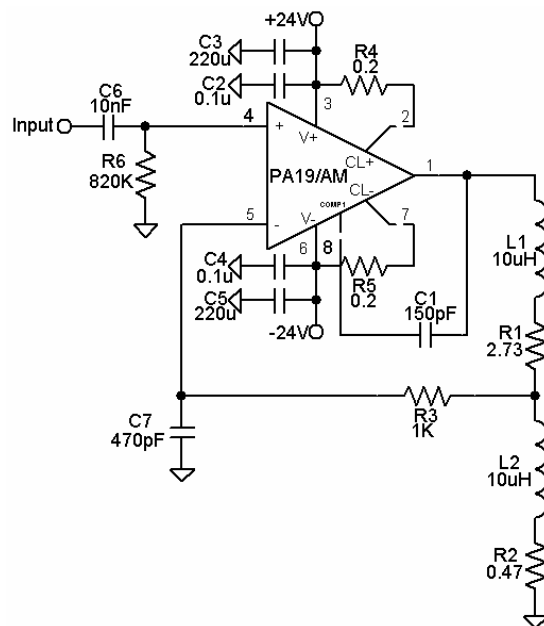


Fig. 4: driving amplifier for one individual TX coil labeled L1

However, the design of a stable wideband current source with power amplifiers is not trivial. Our particular design employs an inductive element (L_2) as current sensing element which, together with the frequency response of the PA's open loop gain $A_0(f)$ provides a high loop gain over a wide frequency band. The output impedance drops from $1 k\Omega$ at 100 kHz to 500Ω at 300 kHz and remains then constant at 500Ω up to 600 kHz. A higher output impedance could not be reached due to stability considerations and limitation of the dynamic input range of the PA.

A particular problem for stability is the parasitic pi-section network which the TX inductance L_1 forms together with the parasitic capacitances of the feeding cables which could not be made shorter than 1m. R_1 and R_2 serve for avoiding purely reactive loads so as to meet the allowable power ratings of the PA19. C_1 and C_7 are compensation capacitances required for maintaining stability.

D. Receiving amplifiers

The receiving circuits are the same as in the previously used prototype. They have been described in detail in [7] therefore just the characteristic data are repeated here. The differential amplifier has a first stage based on the AD797, that has a specified typical input voltage noise density of $0.9 nV/\sqrt{Hz}$, and a second stage based on a Differential Line Driver, the MAX4147. The voltage gain of this stage is 37.5. A differential multiplexer selects sequentially 7 gradiometer signals of the first TRXU plus the reference and then 7 gradiometer signals of the second TRXU plus the same reference. After the multiplexer we have a differential-to-unipolar amplifier with a gain of 2 based on the MAX 435. The digitizer board has 8 converters with a resolution of 12 bits and a conversion rate of up to 60 MSamples/s (NI PXI-5105). Using an input range of $\pm 1V$ the input noise of the ADC board is much smaller than the contribution of the expected thermal noise of previous stages. To achieve 16-channel operation one frame is currently acquired by 1:2 multiplexing of both the transmit coils and the receiving preamplifiers which requires 4 sequential acquisition cycles.

E. Performance measurements

The 8 signals after the multiplexer were acquired at a speed of 10 MSamples/s per channel and with a frame length of 20 ms (200000 points) and a full scale input range of 1V. With the PA switched off the measured spectral noise density at 100 kHz was in the range of $1.5 nV/\sqrt{Hz}$. This value was not increased when switching on the PA without injecting any signal. Referring the specified RMS noise voltage of the digitizer board ($300 \mu V @ 24 MHz$ bandwidth) to the amplifier input this corresponds to

an input noise density of $0.8 \text{ nV}/\sqrt{\text{Hz}}$. Thus the noise is dominated by the gradiometer and the preamplifiers which should yield a theoretical value around $1.3 \text{ nV}/\sqrt{\text{Hz}}$.

Injecting a signal of 100 kHz at $0.2A_s$ with a subcarrier spacing of 300 Hz and using a continuous acquisition (1 frame/s) the spectral noise density at 100 kHz does not exceed $8 \text{ nV}/\sqrt{\text{Hz}}$ for most of the channels. Only the spectral peaks associated with the coils in front of the transmitter yield more than $100 \text{ nV}/\sqrt{\text{Hz}}$. A possible reason is that TX-RX-combinations with high mutual coupling are very sensitive to mechanical vibrations and thermal effects.

III. DISCUSSION

A new 16-channel multifrequency MIT system has been developed which allows fast signal acquisition for in-vivo applications. The TX coils are driven by current sources so as not to perturb the excitation field by coils with low-impedance terminations. However, it must be admitted that the output impedance R_0 of the current sources is still comparatively low, so that the coil reactance is 1% of R_0 at 100 kHz rising up to 10% at 1 MHz. Nevertheless the field perturbation is kept low, especially at low frequencies.

Due to the simultaneous excitation of all TX coils the adjustment of the PGRADs is critical. In the current configuration the excitation currents could not be increased beyond $1.5 A_{\text{eff}}$ at 100 kHz without saturating the receiver amplifiers. Compared with our previous prototype with single-excitation this is a reduction by a factor of approximately 5 and consequently also the SNR is theoretically reduced by about 14 dB. There is, however, still room for improvement to compensate this loss. As the equivalent input noise density is still dominated by the preamplifier noise, the gain of the latter can be reduced by a factor of 2. Hence the current could be raised by the same factor, yielding a plus of 6 dB. The future use of ADCs with higher resolution could add another factor of two per bit of resolution increase. Thus a 14 bit system would definitely allow for reaching even a better SNR than with the current system. One significant advantage is the high acquisition speed of the new system reduces drifts and physiological noise considerably. In vivo imaging was clearly impossible with the old system due to the extremely long acquisition time ($>15 \text{ s}$ per image). The actual effective loss of SNR is therefore not yet clear and should be determined in future evaluations. The frame rate is currently limited by the computation power of the PC but

with high performance computers 10 s^{-1} could be reached. If speed is not of primary interest sampling schemes may be adopted with only few active transmitters at the same time. Then only the receivers in front of the TX coils are saturated, the remaining ones yield valid data even when using higher excitation currents. Alternative gradiometer orientations like in [4] are to be tested for better flux cancellation.

ACKNOWLEDGMENT

This work was supported by the SFB project F32-N18 granted by the Austrian Science Fund.

REFERENCES

1. Griffiths H, Stewart WR and Gough W (1999) Magnetic induction tomography. A measuring system for biological tissues. *Ann NY Acad Sci* 873: 335-345
2. Korjenezky A, Cherepenin V, and Sapetsky S (2000) Magnetic induction tomography: Experimental realization. *Physiol Meas* 21: 89-94
3. Peyton A J et al (1996) An overview of electromagnetic inductance tomography: Description of three different systems. *Meas Sci Technol* 7: 261-271
4. Igney CH, Watson S, et al (2005) Design and performance of a planar-array MIT system with normal sensor alignment *Physiol Meas* 26:S263-S278
5. Ma X, Peyton A et al (2006) Hardware and software design electromagnetic induction tomography (EMT) system for high contrast process applications. *Meas Sci. Technol* 17: 111-118
6. Karbeyaz UB, Gencer NG (2003) Electrical conductivity imaging via contactless measurements: an experimental study. *IEEE Trans Med Imaging*, 22: 627 – 635.
7. Rosell J, Merwa R et al (2006) A multifrequency magnetic induction tomography system using planar gradiometers: data collection and calibration. *Physiol Meas* 27: S271-S280
8. Brunner P, Merwa R et al. (2006) Reconstruction of the shape of conductivity spectra using differential multi-frequency magnetic induction tomography. *Physiol Meas* 27: S237-S248
9. Scharfetter H, Casañas R and Rosell J (2003) Biological Tissue Characterization by Magnetic Induction Spectroscopy (MIS): Requirements and Limitations *IEEE Trans Biomed Eng* 50: 870-80

Address of the corresponding author:

Author: Hermann Scharfetter
 Institute: Inst. Of Medical Engineering
 Street: Kronesgasse 5
 City: Graz
 Country: Austria
 Email: hermann.scharfetter@tugraz.at